BEMD Based Ultrasound Image Speckle Reduction Technique Using Pixel-Wise Wiener Filtering

Bhawna GUPTA, *Vineet KHANDELWAL*

Department of Electronics and Communication Engineering, Jaypee Institute of Information Technology, Sector-62, 201309 Noida, Uttar Pradesh, India

bhawna.gupta@jiit.ac.in, vineet.khandelwal@jiit.ac.in

DOI: 10.15598/aeee.19i2.4100

Article history: Received Jan 30, 2021; Revised Mar 17, 2021; Accepted Apr 01, 2021; Published Jun 30, 2021.

Abstract. *In this paper, an improved Bidimensional Empirical Mode Decomposition (BEMD) based speckle reduction technique for ultrasound images has been proposed. The noisy image has been decomposed into its Intrinsic Mode Functions (IMFs) and a residue. The noise component of the low order IMFs is removed with the pixel-wise Wiener filtering. The image is reconstructed with these filtered low order IMFs, high order IMFs and the residue. The performance of the proposed method has been tested on synthetic as well as real ultrasound images having noise components of different variance. The experimental results show that the proposed algorithm performs better than other existing methods for synthetic images as well as real ultrasound images in terms of various image quality matrices.*

Keywords

BEMD, noise reduction, speckle, ultrasound, Wiener.

1. Introduction

Speckle, which is a multiplicative noise, is an unwanted phenomenon that is present in ultrasound images due to scattering at the time of acquiring the image [1]. Speckle reduction in ultrasound images is an essential step and is targeting improvement in the quality of the image in terms of PSNR (Peak Signal to Noise Ratio), CC (Correlation Coefficient), SNR (Signal to Noise Ratio), FoM (Figure of Merit) and SSIM (Structural SIMilarity) [2]. Due to the high-frequency characteristic of the noise component, the main challenge of speckle reduction technique is that while removing noise the information in the edges should not be lost as this is important for diagnosis. The metric used for measuring the same is the EKI (Edge Keeping Index).

Image denoising specifically speckle reduction in ultrasound images has been studied extensively, and it has been broadly classified into different domains, such as spatial domain techniques, transform domain techniques, and hybrid techniques as shown in Fig. 1. The spatial domain techniques work directly on the image pixels while transform domain technique applies an appropriate transform to convert the image to frequency domain before processing. Furthermore, there are hybrid techniques that are combination of spatial domain and transform domain methods.

The spatial domain techniques use local statistics or information redundancy between similar patches and replace the pixel value by processing the nearby pixel values. Most successful amongst this category are diffusion-based filters like Speckle Reducing Anisotropic Diffusion (SRAD), Detail Preserving Anisotropic Diffusion (DPAD), Perona-Malik's Anisotropic Diffusion (PMAD) [3], [4], [5] and [6], Bilateral filters [7] and [8], and patch-based methods like Non Local Mean filter (NLM) [9], [10], [11] and [12] and Optimized Bayesian Nonlocal Mean filter (OBNLM) [13] and [14]. The similar patch-based methods need to select the candidate patch reasonably so that the removal of noise does not lead to lose of edge information. Therefore, recent work as proposed in [15], [16] and [17] uses modified NLM and BM3D algorithms while trying to preserve the edge information. Wiener filters [18] and [19] are the optimum linear filters, that are widely in use for image processing. Performance of the classical pointwise Wiener filter is enhanced for noise

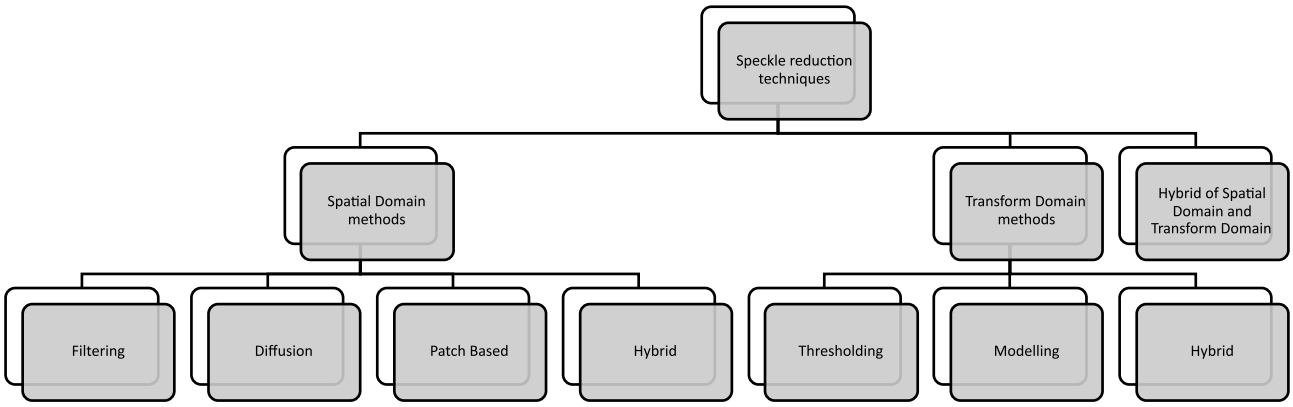

Fig. 1: Classification of Speckle reduction techniques.

corrupted images, with the use of non-local parameter estimation proposed by Andre et al. [20].

Transform domain methods assume that the image can be sparsely represented by its low-frequency components and the speckle is present in the high-frequency components of the image [21]. Thereby, the image high-frequency components are dealt with by applying the thresholding (hard or soft) as in wavelet thresholding method to remove the noise [22]. While these methods give satisfactory results, choosing the right threshold is tricky and should avoid the Gibbs phenomenon and over smoothening effects. Thus, further extension in the transform domain techniques includes data-driven techniques and modeling techniques.

Hybrid techniques are the ones that combine spatial domain methods with transform domain methods for the improvement of denoising performance. Some of the recent hybrid techniques are as introduced in [23], [24] and [25].

Empirical Mode Decomposition (EMD) was introduced by Huang et. al [26] in 1998. This is a very useful algorithm that decomposes the signal in its Intrinsic Mode Functions (IMFs) [27]. This decomposition is done based on their local frequency or oscillation in the spatial domain. Unlike Fourier transform and Wavelet transforms, the basis functions calculated are signal-dependent and are used to estimate a series of IMFs via an iterative procedure called sifting [28].

EMD was introduced in images in 2003 [29] and the Bidimensional Empirical Mode Decomposition (BEMD) for images was introduced in 2005 in [30]. BEMD is also a signal-dependent adaptive technique decomposing the image in a series of IMFs and a residue. The low-order IMFs are the high-frequency components and the high order IMFs are low-frequency components. BEMD is an adaptive multi-resolution analysis technique that is driven by the input signal. Therefore, it is used for various applications in image processing [31].

As the noise in image is mainly concentrated in the high-frequency components, the low order IMFs are having more noise components as compared to the high order IMFs. Accordingly, some BEMD based denoising algorithms use this fact to suppress the noise existing in low order IMFs. But this may not always be true and a significant noise component may also be present in further IMFs as well. Some denoising algorithms deal with this issue and use mutual information [32] or other filtering techniques [33]. These techniques use mutual information or a similarity measure between the probability density functions of the input signal and IMFs, to determine the noise dominant low order IMFs [28], [34] and [35]. These noise-dominant IMFs are discarded and the signal dominant IMFs are retained to obtain the denoised signal. However, most of the high-frequency components of the image also contain detail information such as edges. These algorithms therefore lose important edge details although giving good denoising performance. These details are of importance for diagnostic purposes when dealing with ultrasound images in particular.

This paper introduces an improved technique, in which the low-order high-frequency IMFs, which are noise dominant, are not completely discarded. Rather pixel-based selective filtering in form of Wiener filter is applied to the low order IMFs, to reduce the noise component, while preserving the edge details.

The remainder of the paper is organized as follows. Section 2. , provides a brief overview of BEMD algorithm along with parameter metrics used for comparison. In Sec. 3. , the proposed denoising method is described. The performance evaluation of the proposed method is illustrated in Sec. 4. , and Sec. 5. presents the conclusions.

2. Background

2.1. Bidimensional Empirical Mode Decomposition

EMD in signals was introduced by Huang et. al [26], which is an adaptive technique, which does not have predefined basis functions and decomposes the signal into various IMFs. Similar to EMD in one dimension, BEMD is an adaptive technique being applied to the images [31]. This decomposes the signal into IMFs and a residue. For the sake of illustration, BEMD algorithm is presented here briefly.

Let $f(m,n)$ be the given image. Let $r_l(m,n)$ represent the residue of l-th IMF. To find the next IMF, the residue of the previous IMF is taken as the input. Let $i_{l,k}(m,n)$ be the input image for the generation of an IMF, where the first index is l-th number IMF, $l = 1,\ldots,L$, the second index is k-th iteration of the sifting process, $k = 1,\ldots,K$ and (m,n) being two spatial dimensions.

Step 1: Start with the given image as the input signal. $i_{1,0}(m,n) = f(m,n)$.

Step 2: Extract all local maxima and minima of $i_{l,k}(m,n)$.

Step 3: Interpolate all local maxima to get the upper envelope $e_u(m,n)$ and interpolate all local minima to get the lower envelope $e_l(m,n)$. The application-specific spline can be used for interpolation.

Step 4: Calculate the envelope mean $\overline{e}_{l,k}(m,n)$ of the upper and the lower envelopes obtained in step 3:

$$\overline{e}_{l,k}(m,n) = \frac{e_u(m,n) + e_l(m,n)}{2}. \tag{1}$$

Step 5: The input signal is updated by subtracting the envelope mean $\overline{e}_{l,k}(m,n)$ for the next iteration:

$$i_{l,k}(m,n) = i_{l,k-1}(m,n) - \overline{e}_{l,k}(m,n), \quad k \to k+1. \tag{2}$$

Step 6: This step is to check if the result obtained in step 5 is an IMF or not. For this standard deviation, ϵ is calculated as:

$$\epsilon = \sum_{m=0}^{M-1}\sum_{n=0}^{N-1} \frac{|i_{l,k}(m,n) - i_{l,k-1}(m,n)|^2}{i^2_{l,k-1}(m,n)}. \tag{3}$$

Step 7: Check the standard deviation ϵ to be less than a predefined value (generally 0.2–0.3). If the value is greater than the criterion, repeat steps 2–6. When the value of ϵ is below the predefined value, the result of step 5 is the required l-th IMF, $f_l(m,n)$:

$$f_l(m,n) = i_{l,k}(m,n). \tag{4}$$

Step 8: The residue of the l-th IMF is defined as:

$$r_l(m,n) = i_{l,0}(m,n) - f_l(m,n). \tag{5}$$

Step 9: The next IMF is calculated by taking the residue calculated as the input signal and starting over from step 2:

$$i_{l+1,0}(m,n) = r_l(m,n). \tag{6}$$

All subsequent IMFs are calculated by repeating the steps from 2–9. The process is stopped when the residue calculated has no more extrema. So, with the total L number of IMFs calculated and the last residue without extrema r_L, the original signal can be represented as:

$$f(m,n) = \sum_{l=1}^{L} f_l(m,n) + r_L(m,n). \tag{7}$$

It is important to mention here that the low order IMFs, are corresponding to the high frequency while the high order IMFs are corresponding to the low frequency.

2.2. Image Quality Performance Metrics

The performance of the proposed BEMD based noise reduction technique using a Wiener filter is analyzed and compared both quantitatively and qualitatively with the existing techniques. For synthetic US images generated using Field II software [36] developed by J. A. Jensen, a quantitative analysis is carried out using performance metrics viz., Peak Signal to Noise Ratio (PSNR) [37], Edge Keeping Index (EKI) [38], Structure SIMilarity Index Measures (SSIM) [39], Correlation Coefficient (CC) [40], Signal to Noise Ratio (SNR) [37] and Figure of Merit (FoM) [41]. However, for real ultrasound images, as no noise-free image is available, the Mean to Variance Ratio (MVR) [42] and an Equivalent Number of Looks (ENL) [43] are used for quantitative evaluation. For a noisy image $f(m,n)$ and the reconstructed denoised image $f_r(m,n)$, the metrics used for quantitative evaluation are defined as follows:

- Peak Signal to Noise Ratio (PSNR) is a frequently used measure to access the efficacy of the denoising algorithm. It is the ratio of peak signal power to the noise power given by Eq. (8), where $l = 255$ for an 8-bit grayscale image of size $M \times N$.
- Edge Keeping Index (EKI) is a parameter to measure the edge keeping capability of a denoising algorithm, see Eq. (9), where Δf and Δf_r are high pass filtered version of f and f_r, respectively, obtained using 3×3 Laplacian operator and $\overline{\Delta f}$ and

$$\mathrm{PSNR} = 10\log_{10}\frac{l^2}{\frac{1}{MN}\sum_{m=0}^{M-1}\sum_{n=0}^{N-1}\left(f(m,n)-f_r(m,n)\right)^2}, \tag{8}$$

$$\mathrm{EKI} = \frac{\sum_{m=0}^{M-1}\sum_{n=0}^{N-1}\left(\Delta f(m,n)-\Delta\overline{f}\right)\left(\Delta f_r(m,n)-\Delta\overline{f_r}\right)}{\sqrt{\sum_{n=0}^{N-1}\left(\Delta f(m,n)-\Delta\overline{f}\right)^2\left(\Delta f_r(m,n)-\Delta\overline{f_r}\right)^2}}, \tag{9}$$

$$\mathrm{CC} = \frac{\sum_{m=0}^{M-1}\sum_{n=0}^{N-1}\left(f(m,n)-\overline{f}\right)\left(f_r(m,n)-\overline{f_r}\right)}{\sqrt{\left(\sum_{m=0}^{M-1}\sum_{n=0}^{N-1}\left(f(m,n)-\overline{f}\right)^2\right)\left(\sum_{m=0}^{M-1}\sum_{n=0}^{N-1}\left(f_r(m,n)-\overline{f_r}\right)^2\right)}}. \tag{12}$$

$\overline{\Delta f_r}$ are the mean values of Δf and Δf_r, respectively.

- Structural SIMilarity (SSIM) is for measuring the structure saving capability of the denoising algorithm. If $\overline{f}$ and $\overline{f_r}$ are the mean and σ_i and σ_{ir} are the standard deviation of original and reconstructed images respectively, then:

$$\mathrm{SSIM} = \frac{\left(2\overline{f}(m,n)\overline{f_r}(m,n)+c_1\right)\left(2\sigma_{f,f_r}+c_2\right)}{\left(\overline{f}^2+\overline{f_r}^2+c_1\right)\left(\sigma_i^2+\sigma_{f,f_r}^2+c_2\right)}, \tag{10}$$

where $c_1 = (0.01l)^2$, $c_2 = (0.03l)^2$ and covariance image matrix is given by:

$$\sigma_{f,f_r}^2 = \frac{1}{N-1}\sum_{k=0}^{N-1}\left(f_k-\overline{f}\right)\left(f_{rk}-\overline{f_r}\right). \tag{11}$$

- Correlation Coefficient (CC) defines the interdependence of the noisy image and the reconstructed image. It is defined as shown in Eq. (12).
- Signal to Noise Ratio (SNR) is defined as the ratio of signal power to noise power:

$$\mathrm{SNR} = 10\log_{10}\frac{\sum_{m=0}^{M-1}\sum_{n=0}^{N-1}\left(f(m,n)\right)^2}{\sqrt{\sum_{m=0}^{M-1}\sum_{n=0}^{N-1}\left(f(m,n)-f_r(m,n)\right)^2}}. \tag{13}$$

- Figure of Merit (FoM) defined by Eq. (14) is a measure of preserving the edge information while denoising the image:

$$\mathrm{FoM} = \frac{1}{\max\left(N_D,N_I\right)}\sum_{n=1}N_D\left(\frac{1}{1+\gamma d_n^2}\right), \tag{14}$$

where N_D and N_I are the numbers of edge pixels that are detected and ideally present respectively; d_n is the Euclidean distance between the n-th detected edge pixel and the closest ideal pixel that is present; γ is a scalar usually equal to $\frac{1}{9}$ for image calculations.

- Mean to Variance Ratio (MVR) is calculated for real images for a selected local region as:

$$\mathrm{MVR} = \frac{\mu_l}{\sigma_l^2}, \tag{15}$$

where μ_l and σ_l^2 are the local mean and variance.

- Equivalent Number of Looks (ENL) is another parameter used for real images. It is the ratio of the square of mean to the variance for a selected local region given by:

$$\mathrm{ENL} = \frac{\mu_l^2}{\sigma_l^2}. \tag{16}$$

3. BEMD Based Pixel-Wise Wiener Filtering

In this section, the proposed BEMD based speckle reduction in Ultrasound images using Wiener filtering has been introduced. Due to the high-frequency characteristics of the speckle noise, it is mainly constrained in the low order IMFs of the ultrasound image. Therefore, considering the low order IMFs for noise reduction is the choice that has been considered.

At the same time, the edge information is also a piece of crucial information from the point of view of the diagnostic importance in ultrasound images. As the edges are signified by the abrupt changes in the amplitude in the spatial domain, the low order IMFs cannot be discarded all together. The proposed scheme utilizes the fact that low order IMFs has maximum noise

component and thus low pass filters these IMFs using an adaptive Wiener filter for preserving the edge information present in these low order IMFs.

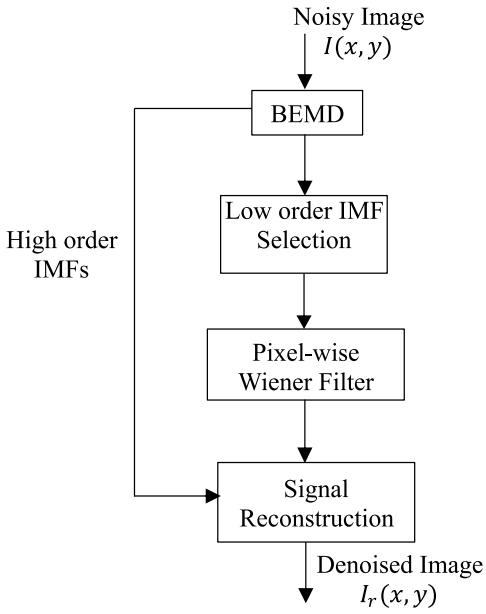

Fig. 2: Block Diagram of the proposed scheme.

The steps in the proposed algorithm are as follows:

Step 1: Calculate the BEMD of the ultrasound image corrupted with speckle noise.

Step 2: Select the low order IMFs which have the high-frequency components and are therefore having both the noise and the edge information.

Step 3: Calculate the pixel-wise Wiener filtering of the selected IMFs [44] assuming additive noise $v(n_1, n_2)$ with zero mean and variance σ_v^2. Wiener filter estimates the local mean and variance around each pixel of the chosen IMF:

$$\mu_e = \frac{1}{NM} \sum_{m,n \in w} f_l(m,n), \tag{17}$$

$$\sigma_e^2 = \frac{1}{NM} \sum_{m,n \in w} f_l^2(m,n) - \mu_e^2, \tag{18}$$

where w is the window corresponding to the $N \times M$ neighborhood of each pixel in the IMF. This filter then creates a pixel-wise estimate given as:

$$f_e(m,n) = \mu_e + \frac{\sigma_e^2 - \sigma_v^2}{\sigma_e^2} \left(f_l(m,n) - \mu_e \right). \tag{19}$$

Step 4: The low-order filtered IMFs combined with the high-order IMFs and the residue are used to reconstruct the denoised image.

4. Experimental Results

The kidney and fetus Field II images have been simulated and used for the experiments performed on MATLAB. The speckle noise has been added to the image with $\sigma^2 = 0.1$, $\sigma^2 = 0.2$, and $\sigma^2 = 0.3$.

Figure 3 shows the BEMD IMFs for synthetic kidney image and synthetic fetus image, that are obtained for noise variance $\sigma^2 = 0.1$. The spline interpolation that is used in our case is a cubic spline. As can be seen in Fig. 3, the low order IMFs are having only the high-frequency components corresponding to speckle and edges. The Wiener filter is best defined for additive noise. Therefore, the multiplicative speckle noise has been log-transformed and converted to additive noise before applying BEMD.

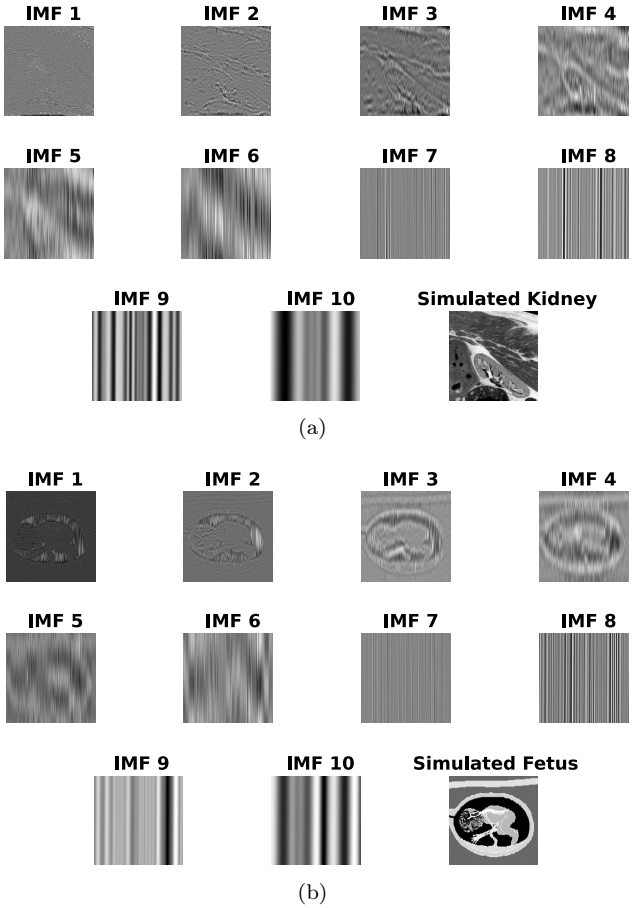

Fig. 3: BEMD IMFs for (a) Syntetic Kidney Field II image and (b) Synthetic Fetus Field II image.

Pixel-wise Wiener filtering has been applied on low order IMFs. It has been observed that the results were best for the Wiener filter applied to IMF1 and IMF2. While applying Wiener filtering, 8-neighborhood has been utilized for calculation of local region.

The Wiener filtered IMFs along with higher-order IMFs and the residue is reconstructed to get the de-

Tab. 1: Correlation Coefficient (CC) for various techniques.

Technique	CC					
	Noise variance σ^2					
	Synthetic fetus image			Synthetic kidney image		
	0.1	0.2	0.3	0.1	0.2	0.3
Proposed EMD	**0.96234**	**0.94607**	**0.92693**	**0.94284**	**0.90968**	**0.87969**
Conventional EMD	0.95102	0.92555	0.87480	0.92645	0.87332	0.81060
Bilateral	0.91368	0.84291	0.78464	0.84947	0.74776	0.67000
SRAD	0.94191	0.87916	0.81739	0.91540	0.8292	0.75551
NLM	0.93126	0.87093	0.82044	0.87618	0.78484	0.71328
OBNLM	0.95155	0.90697	0.86630	0.90923	0.83734	0.77571
PMAD	0.94638	0.88481	0.82668	0.90595	0.80801	0.72333

Tab. 2: Signal to Noise Ratio (SNR) for various techniques.

Technique	SNR					
	Noise variance σ^2					
	Synthetic fetus image			Synthetic kidney image		
	0.1	0.2	0.3	0.1	0.2	0.3
Proposed EMD	**14.0620**	**12.6740**	**11.4590**	**15.6020**	**13.6940**	**12.4430**
Conventional EMD	13.9140	11.0110	10.2900	14.2440	12.0820	10.2030
Bilateral	10.7200	7.9790	6.4897	10.7320	8.0182	6.5425
SRAD	12.6000	9.2820	7.3429	13.7580	10.2860	8.4398
NLM	11.7240	8.8585	7.3089	11.7650	8.9261	7.3852
OBNLM	13.3050	10.3730	8.6871	13.3320	10.4920	8.8753
PMAD	12.9410	9.4890	7.5779	13.2020	9.6131	7.6633

Tab. 3: Figure of Merit (FoM) for various techniques.

Technique	FoM					
	Noise variance σ^2					
	Synthetic fetus image			Synthetic kidney image		
	0.1	0.2	0.3	0.1	0.2	0.3
Proposed EMD	0.82919	**0.86146**	**0.84317**	0.86334	**0.86188**	**0.82560**
Conventional EMD	0.82761	0.84320	0.82133	0.86112	0.83281	0.81143
Bilateral	0.81285	0.74764	0.70383	0.77549	0.72620	0.69278
SRAD	0.86349	0.78487	0.73090	0.83815	0.75237	0.73401
NLM	0.87531	0.79219	0.75194	0.83151	0.78397	0.74317
OBNLM	**0.89364**	0.84390	0.80875	**0.88295**	0.78922	0.76806
PMAD	0.86438	0.79341	0.73724	0.85802	0.76742	0.71880

noised image. The qualitative assessment is shown in Fig. 4 for synthetic kidney and in Fig. 5 for synthetic fetus for the noise of variance $\sigma^2 = 0.1$. As can be seen, the denoised image is perceptually of the same quality as that of the original image.

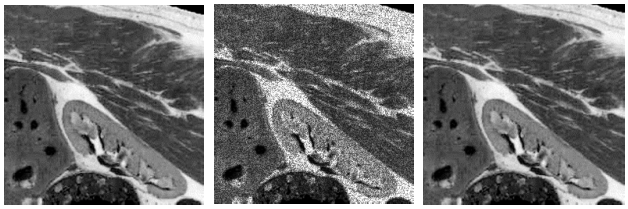

(a) (b) (c)

Fig. 4: Synthetic kidney for $\sigma^2 = 0.1$: (a) original image, (b) noisy image and (c) denoised image.

Table 1, Tab. 2, Tab. 3, Tab. 4, Tab. 5 and Tab. 6 shows the comparison of various parameters obtained for different values of σ for the two Field II synthetic images, fetus and kidney. As can be seen, the proposed

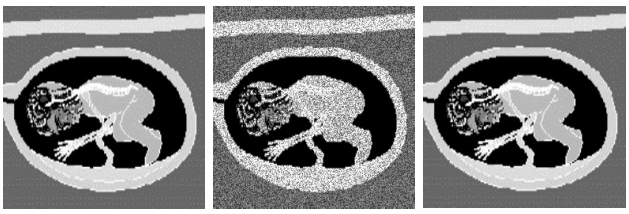

(a) (b) (c)

Fig. 5: Synthetic fetus for $\sigma^2 = 0.1$: (a) original image, (b) noisy image and (c) denoised image.

algorithm performs better than the existing techniques in terms of PSNR, SNR, and CC, for noise variance $\sigma^2 = 0.1$. The results obtained for these parameters give similar results even at higher noise variances, $\sigma^2 = 0.2$ and $\sigma^2 = 0.3$.

Moreover, the result in the tables show that the proposed technique gives comparable results with the existing techniques in terms of EKI, SSIM, and FoM for

Tab. 4: Peak Signal to Noise Ratio (PSNR) for various techniques.

Technique	PSNR					
	Noise variance σ^2					
	Synthetic fetus image			Synthetic kidney image		
	0.1	0.2	0.3	0.1	0.2	0.3
Proposed EMD	**24.946**	**23.577**	**22.383**	**24.322**	**22.388**	**21.158**
Conventional EMD	22.398	20.671	20.330	22.317	20.672	19.821
Bilateral	21.056	18.009	16.260	19.025	15.992	14.254
SRAD	23.058	19.463	17.260	22.192	18.459	16.398
NLM	22.336	19.310	17.594	20.288	17.239	15.518
OBNLM	24.002	21.030	19.306	21.971	19.054	17.350
PMAD	23.539	19.837	17.690	21.730	17.878	15.686

Tab. 5: Edge Keeping Index (EKI) for various techniques.

Technique	EKI					
	Noise variance σ^2					
	Synthetic fetus image			Synthetic kidney image		
	0.1	0.2	0.3	0.1	0.2	0.3
Proposed EMD	**0.64603**	**0.59358**	**0.53587**	0.54885	**0.50024**	**0.49630**
Conventional EMD	0.61720	0.52081	0.50012	0.51320	0.48230	0.45321
Bilateral	0.59360	0.54006	0.52306	0.53703	0.49294	0.47574
SRAD	0.55134	0.49815	0.49498	0.49201	0.45619	0.43757
NLM	0.59768	0.54228	0.51775	0.53614	0.49024	0.47184
OBNLM	0.62562	0.54757	0.52198	**0.55135**	0.49023	0.46734
PMAD	0.55606	0.50568	0.49567	0.49833	0.46407	0.44813

Tab. 6: Structural SIMilarity (SSIM) for various techniques.

Technique	SSIM					
	Noise variance σ^2					
	Synthetic fetus image			Synthetic kidney image		
	0.1	0.2	0.3	0.1	0.2	0.3
Proposed EMD	0.70575	0.66684	**0.62823**	0.61088	**0.53961**	**0.49747**
Conventional EMD	0.72345	0.65482	0.61291	0.61098	0.49308	0.45320
Bilateral	0.71808	0.61478	0.5552	0.53328	0.39544	0.32945
SRAD	0.76831	0.67000	0.59414	**0.65411**	0.50453	0.41941
NLM	0.74678	0.64120	0.58082	0.56396	0.42391	0.35323
OBNLM	**0.78688**	**0.68623**	0.62356	0.62079	0.47589	0.39955
PMAD	0.78014	0.68009	0.60847	0.63845	0.47608	0.38675

$\sigma^2 = 0.1$. At the same time, based on the analysis of the values obtained by the experiments, the scheme is giving better results in terms of these parameters for higher values of $\sigma^2 = 0.2$ and $\sigma^2 = 0.3$. Thus, we can summarize that the technique performs acceptably well even at higher noise levels.

For completeness of the efficacy evaluation of the proposed algorithm, an experiment has also been performed on the real ultrasound image database taken from [45]. The real images have three sets of data namely kidney, liver, and gall bladder images each having around 85 images. Three regions were selected randomly for all three sets and the MVR and ENL have been calculated.

Figure 6(a) shows the real liver ultrasound image and the three regions that are taken for calculations of MVR and ENL. Figure 6(b) and Fig. 6(c) are the results that are obtained for the selected regions. Table 7 shows the MVR and ENL for the real liver ultrasound database.

Similar experiments were also performed on real ultrasound image data sets of kidney and gall bladder, however, due to paucity of space we have shown MVR and ENL plots for liver database only. The results obtained for the other sets are also in conjunction with the results shown here.

Tab. 7: MVR and ENL for Real Liver Ultrasound Database.

Technique	MVR	ENL
Proposed EMD	18.51 ± 3.76	5.25 ± 2.79
Conventional BEMD	17.91 ± 5.32	5.01 ± 2.54
Bilateral	15.42 ± 5.16	3.96 ± 2.32
SRAD	17.66 ± 4.52	4.87 ± 2.35
NLM	17.01 ± 4.14	4.91 ± 2.15
OBNLM	17.81 ± 4.71	4.95 ± 2.61
PMAD	16.39 ± 6.21	4.33 ± 2.79

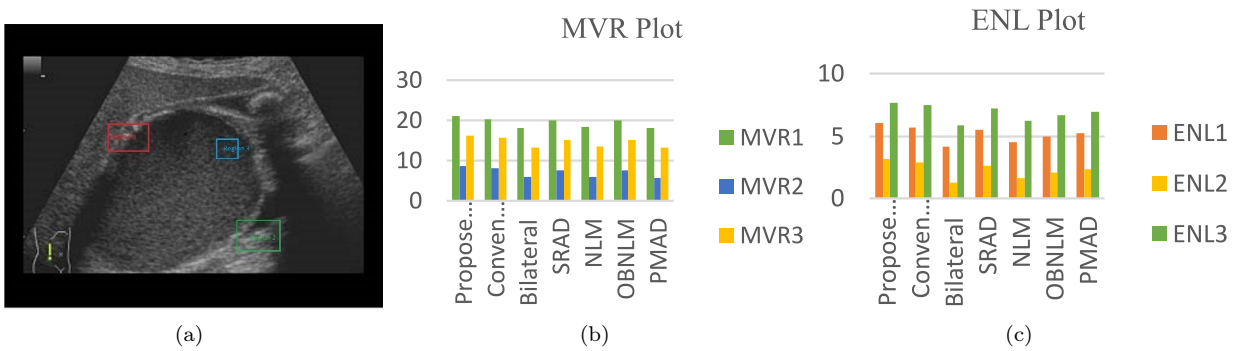

Fig. 6: (a) Real liver image with selected regions, (b) MVR plot, (c) ENL plot.

5. Conclusion

In this paper, a BEMD based image denoising algorithm using pixel-wise Wiener filtering has been presented. The proposed method solves the problem of losing the edge information in the conventional BEMD based denoising technique. The conventional BEMD based algorithm is able to remove low order IMF, but loses important edge information which has been preserved with the help of the method proposed herein. The performance of the method has been verified quantitatively in terms of PSNR, EKI, SSIM, FoM, SNR, and CC for synthetic ultrasound images. The quantitative analysis is also done on the real ultrasound images in terms of MVR and ENL. It has been found that the proposed algorithm performs better than many other existing state-of-the-art techniques and can preserve the edge information.

Author Contributions

V.K. conceived the presented idea. B.G. developed the theory and performed the experiments. V.K. encouraged B.G. to investigate and supervised the findings of this work. Both authors discussed the results and contributed to the final manuscript.

References

[1] BURCKHARDT, C. B. Speckle in ultrasound B-mode scans. *IEEE Transactions on Sonics and Ultrasonics*. 1978, vol. 25, iss. 1, pp. 1–6. ISSN 2162-1403. DOI: 10.1109/T-SU.1978.30978.

[2] SZABO, T. L. *Diagnostic Ultrasound Imaging: Inside Out*. 2nd ed. Amsterdam: Academic Press, 2014. ISBN 978-012-396487-8.

[3] YU, Y. and S. T. ACTON. Speckle reducing anisotropic diffusion. *IEEE Transactions on Image Processing*. 2002, vol. 11, iss. 11, pp. 1260–1270. ISSN 1941-0042. DOI: 10.1109/TIP.2002.804276.

[4] RAHIMI, M. and M. YAZDI. A new hybrid algorithm for speckle noise reduction of SAR images based on mean-median filter and SRAD method. In: *2015 2nd International Conference on Pattern Recognition and Image Analysis (IPRIA)*. Rasht: IEEE, 2015, pp. 1–6. ISBN 978-1-4799-8445-9. DOI: 10.1109/PRIA.2015.7161623.

[5] LIU, X., J. LIU, X. XU, L. CHUN, J. TANG and Y. DENG. A robust detail preserving anisotropic diffusion for speckle reduction in ultrasound images. In: *The 2010 International Conference on Bioinformatics and Computational Biology (BIOCOMP 2010): Genomics*. Las Vegas: BMC Genomics, 2011, pp. 1–10. DOI: 10.1186/1471-2164-12-S5-S14.

[6] PERONA, P. and J. MALIK. Scale-space and edge detection using anisotropic diffusion. *IEEE Transactions on Pattern Analysis and Machine Intelligence*. 1990, vol. 12, iss. 7, pp. 629–639. ISSN 1939-3539. DOI: 10.1109/34.56205.

[7] TOMASI, C. and R. MANDUCHI. Bilateral filtering for gray and color images. In: *Sixth International Conference on Computer Vision*. Bombay: IEEE, 1998, pp. 839–846. ISBN 81-7319-221-9. DOI: 10.1109/ICCV.1998.710815.

[8] BALOCCO, S., C. GATTA, O. PUJOL, J. MAURI and P. RADEVA. SRBF: Speckle Reducing Bilateral Filtering. *Ultrasound in Medicine & Biology*. 2010, vol. 36, iss. 8, pp. 1353–1363. ISSN 1879-291X. DOI: 10.1016/j.ultrasmedbio.2010.05.007.

[9] COUPE, P., P. HELLIER, C. KERVRANN and C. BARILLOT. Nonlocal means-based speckle filtering for ultrasound images. *IEEE Transactions on Image Processing*. 2009,

vol. 18, iss. 10, pp. 2221–2229. ISSN 1941-0042. DOI: 10.1109/TIP.2009.2024064.

[10] ZHAN, Y., M. DING, L. WU and X. ZHANG. Nonlocal means method using weight refining for despeckling of ultrasound images. *Signal Processing*. 2014, vol. 103, iss. 1, pp. 201–213. ISSN 1872-7557. DOI: 10.1016/j.sigpro.2013.12.019.

[11] LI, X., H. HE, R. WANG and J. CHENG. Superpixel-guided nonlocal means for image denoising and super-resolution. *Signal Processing*. 2016, vol. 124, iss. 1, pp. 173–183. ISSN 1872-7557. DOI: 10.1016/j.sigpro.2015.09.021.

[12] GUO, Y., Y. WANG and T. HOU. Speckle filtering of ultrasonic images using a modified non local-based algorithm. *Biomedical Signal Processing and Control*. 2011, vol. 6, iss. 2, pp. 129–138. ISSN 1746-8108. DOI: 10.1016/j.bspc.2010.10.004.

[13] KERVRANN, C., J. BOULANGER and P. COUPE. Bayesian Non-local Means Filter, Image Redundancy and Adaptive Dictionaries for Noise Removal. In: *SSVM: International Conference on Scale Space and Variational Methods in Computer Vision*. Ischia: Springer, 2007, pp. 520–532. ISBN 978-3-540-72823-8. DOI: 978-3-540-72823-8_45.

[14] COUPE, P., P. HELLIER, C. KERVRANN and C. BARILLOT. Bayesian non local means-based speckle filtering. In: *2008 5th IEEE International Symposium on Biomedical Imaging: From Nano to Macro*. Paris: IEEE, 2008, pp. 1291–1294. ISBN 978-1-4244-2002-5. DOI: 10.1109/ISBI.2008.4541240.

[15] YANG, J., J. FAN, D. AI, X. WANG, Y. ZHENG, S. TANG and Y. WANG. Local statistics and non-local mean filter for speckle noise reduction in medical ultrasound image. *Neurocomputing*. 2016, vol. 195, iss. 1, pp. 88–95. ISSN 1872-8286. DOI: 10.1016/j.neucom.2015.05.140.

[16] MEI, F., D. ZHANG and Y. YANG. Improved non-local self-similarity measures for effective speckle noise reduction in ultrasound images. *Computer Methods and Programs in Biomedicine*. 2020, vol. 196, iss. 1, pp. 1–14. ISSN 1872-7565. DOI: 10.1016/j.cmpb.2020.105670.

[17] HUANG, S., C. TANG, M. XU, Y. QIU, and Z. LEI. BM3D-based total variation algorithm for speckle removal with structure-preserving in OCT images. *Applied Optics*. 2019, vol. 58, iss. 23, pp. 6233–6243. ISSN 2155-3165. DOI: 10.1364/AO.58.006233.

[18] JADWA, S. Wiener Filter based Medical Image De-noising. *International Journal of Science and Engineering Applications*. 2018, vol. 7, iss. 9, pp. 318–323. ISSN 2319-7560. DOI: 10.7753/IJSEA0709.1014.

[19] KAY, S. M. *Fundamentals of Statistical Processing, Volume I*. 1st ed. Englewood Cliffs: Prentice Hall PTR, 1993. ISBN 978-0-1334-5711-7.

[20] BINDILATTI, A. A., M. A. C. VIEIRA and N. D. A. MASCARENHAS. Poisson Wiener filtering with non-local weighted parameter estimation using stochastic distances. *Signal Processing*. 2018, vol. 144, iss. 1, pp. 68–76. ISSN 1872-7557. DOI: 10.1016/j.sigpro.2017.10.001.

[21] JAIN, P. and V. TYAGI. A survey of edge-preserving image denoising methods. *Information Systems Frontiers*. 2016, vol. 18, iss. 1, pp. 159–170. ISSN 1572-9419. DOI: 10.1007/s10796-014-9527-0.

[22] DONOHO, D. L. De-noising by soft-thresholding. *IEEE Transactions on Information Theory*. 1995, vol. 41, iss. 3, pp. 613–627. ISSN 1557-9654. DOI: 10.1109/18.382009.

[23] CHOI, H. and J. JEONG. Speckle Noise Reduction Technique for SAR Images Using Statistical Characteristics of Speckle Noise and Discrete Wavelet Transform. *Remote Sensing*. 2019, vol. 11, iss. 10, pp. 1184–1210. ISSN 2072-4292. DOI: 10.3390/rs11101184.

[24] CHOI, H. and J. JEONG. Despeckling Algorithm for Removing Speckle Noise from Ultrasound Images. Symmetry. 2020, vol. 12, iss. 6, pp. 938–963. ISSN 2073-8994. DOI: 10.3390/sym12060938.

[25] CHEN, Y., M. ZHANG, H.-M. YAN, Y.-J. LI and K.-F. Yang. A New Ultrasound Speckle Reduction Algorithm Based on Superpixel Segmentation and Detail Compensation. *Applied Sciences*. 2019, vol. 9, iss. 8, pp. 1693–1705. ISSN 2076-3417. DOI: 10.3390/app9081693.

[26] HUANG, N. E., Z. SHEN, S. R. LONG, M. C. WU, H. H. SHIH, Q. ZHENG, N.-C. YEN, C. C. TUNG and H. H. LIU. The empirical mode decomposition and the Hilbert spectrum for nonlinear and non-stationary time series analysis. *Proceedings of the Royal Society A: Mathematical, Physical and Engineering Sciences*. 1998, vol. 454, iss. 1971, pp. 903–995. ISSN 1471-2946. DOI: 10.1098/rspa.1998.0193.

[27] LINDERHED, A. Image Empirical Mode Decomposition: a New Tool for Image Processing. *Advances in Adaptive Data Analysis*. 2009, vol. 1, iss. 2, pp. 265–294. ISSN 1793-7175. DOI: 10.1142/S1793536909000138.

[28] KOPSINIS, Y. and S. MCLAUGHLIN. Development of EMD-Based Denoising Methods Inspired by Wavelet Thresholding. *IEEE Transactions on Signal Processing*. 2009, vol. 57, iss. 4, pp. 1351–1362. ISSN 1941-0476. DOI: 10.1109/TSP.2009.2013885.

[29] NUNES, J. C., Y. BOUAOUNE, E. DELECHELLE, O. NIANG and P. BUNEL. Image analysis by bidimensional empirical mode decomposition. *Image and Vision Computing*. 2003, vol. 21, iss. 12, pp. 1019–1026. ISSN 1872-8138. DOI: 10.1016/S0262-8856(03)00094-5.

[30] NUNES, J. C., S. GUYOT and E. DELECHELLE. Texture analysis based on local analysis of the Bidimensional Empirical Mode Decomposition. *Machine Vision and Applications*. 2005, vol. 16, iss. 3, pp. 177–188. ISSN 1432-1769. DOI: 10.1007/s00138-004-0170-5.

[31] AN, F.-P., D.-C. LIN, X.-W. ZHOU and Z. SUN. Enhancing Image Denoising Performance of Bidimensional Empirical Mode Decomposition by Improving the Edge Effect. *International Journal of Antennas and Propagation*. 2015, vol. 2015, iss. 1, pp. 1–13. ISSN 1687-5877. DOI: 10.1155/2015/769478.

[32] OMITAOMU, O. A., V. A. PROTOPOPESCU and A. R. GANGULY. Empirical Mode Decomposition Technique With Conditional Mutual Information for Denoising Operational Sensor Data. *IEEE Sensors Journal*. 2011, vol. 11, iss. 10, pp. 2565–2575. ISSN 1558-1748. DOI: 10.1109/JSEN.2011.2142302.

[33] KOMATY, A., A.-O. BOUDRAA, B. AUGIER and D. DARE-EMZIVAT. EMD-Based Filtering Using Similarity Measure Between Probability Density Functions of IMFs. *IEEE Transactions on Instrumentation and Measurement*. 2014, vol. 63, iss. 1, pp. 27–34. ISSN 1557-9662. DOI: 10.1109/TIM.2013.2275243.

[34] LIU, D. and X. CHEN. Image denoising based on improved bidimensional empirical mode decomposition thresholding technology. *Multimedia Tools and Applications*. 2019, vol. 78, iss. 6, pp. 7381–7417. ISSN 1573-7721. DOI: 10.1007/s11042-018-6503-6.

[35] AN, F.-P. and X.-W. ZHOU. BEMD–SIFT feature extraction algorithm for image processing application. *Multimedia Tools Applications*. 2017, vol. 76, iss. 11, pp. 13153–13172. ISSN 1573-7721. DOI: 10.1007/s11042-016-3746-y.

[36] JENSEN, J. A. FIELD: A program for simulating ultrasound systems. *Medical & Biological Engineering & Computing*. 1996, vol. 34, iss. 1, pp. 351–352. ISSN 1741-0444.

[37] MATEO, J. L. and A. FERNANDEZ-CABALLERO. Finding out general tendencies in speckle noise reduction in ultrasound images. *Expert Systems with Applications*. 2009, vol. 36, iss. 4, pp. 7786–7797. ISSN 1873-6793. DOI: 10.1016/j.eswa.2008.11.029.

[38] NASRI, M. and H. NEZAMABADI-POUR. Image denoising in the wavelet domain using a new adaptive thresholding function. *Neurocomputing*. 2009, vol. 72, iss. 4, pp. 1012–1025. ISSN 1872-8286. DOI: 10.1016/j.neucom.2008.04.016.

[39] WANG, Z., A. C. BOVIK, H. R. SHEIKH and E. P. SIMONCELLI. Image quality assessment: from error visibility to structural similarity. *IEEE Transactions on Image Processing*. 2004, vol. 13, iss. 4, pp. 600–612. ISSN 1941-0042. DOI: 10.1109/TIP.2003.819861.

[40] RODGERS, J. L. and W. A. NICEWANDER. Thirteen Ways to Look at the Correlation Coefficient. *The American Statistician*. 1988, vol. 42, iss. 1, pp. 59–66. ISSN 1537-2731. DOI: 10.1080/00031305.1988.10475524.

[41] PRATT, W. K. *Digital Image Processing: PIKS Scientific Inside*. 4th ed. New York: John Wiley & Sons, 2007. ISBN 978-0-471-76777-0.

[42] NAGAO, M. and T. MATSUYAMA. Edge preserving smoothing. *Computer Graphics and Image Processing*. 1979, vol. 9, iss. 4, pp. 394–407. ISSN 1557-9697. DOI: 10.1016/0146-664X(79)90102-3.

[43] BHUIYAN, M. I. H., M. O. AHMAD and M. N. S. SWAMY. Spatially adaptive thresholding in wavelet domain for despeckling of ultrasound images. *IET Image Processing*. 2009, vol. 3, iss. 3, pp. 147–162. ISSN 1751-9667. DOI: 10.1049/iet-ipr.2007.0096.

[44] LIM, J. S. *Two-Dimensional Signal and Image Processing*. 1st ed. Upper Saddle River: Prentice Hall PTR, 1990. ISBN 978-0-13-935322-2.

[45] Image Database. *Ultrasound Cases* [online]. Available at: `https://www.ultrasoundcases.info`.

About Authors

Bhawna GUPTA joined the Department of Electronics and Communication Engineering, Jaypee

Institute of Information Technology, Noida, in 2003 and is currently working as Assistant Professor. She received her B.Tech. and M.Tech. degree from Aligarh Muslim University (AMU), Aligarh, India, in the year 2001 and 2003, respectively. She is currently pursuing Ph.D. from Jaypee Institute of Information Technology, Noida, India in area of image processing. Her research interests include biomedical signal processing and digital signal processing.

Vineet KHANDELWAL is working as Associate Professor at the Department of Electronics and Communication Engineering, Jaypee Institute of Information Technology, Noida. He received his Ph.D. degree from School of Computer Systems and Sciences, Jawaharlal Nehru University, New Delhi, India and M.Tech. in Signal Processing from Netaji Subhas University of Technology, New Delhi, India. He obtained his B.E. degree in Electronics and Communication Engineering from Madhav Institute of Technology & Science, Gwalior. His research interest includes signal processing, biomedical signal processing and RF & Optical wireless communication etc.